Journal of Power Sources 195 (2010) 7202–7206

Contents lists available at ScienceDirect

Journal of Power Sources

journal homepage: www.elsevier.com/locate/jpowsour

Study of CoO as an anode catalyst for a membraneless direct borohydride fuel cell

Sai Li, Yongning Liu*, Yan Liu, Yuanzhen Chen

State Key Laboratory for Mechanical Behavior of Materials, School of Materials Science and Eng., Xi'an Jiaotong University, Xi'an 710049, PR China

ARTICLE INFO

Article history:
Received 11 April 2010
Received in revised form 8 May 2010
Accepted 10 May 2010
Available online 31 May 2010

Keywords:
Direct borohydride fuel cell
Cobalt(II) oxide
Cell performance

ABSTRACT

In this paper, cobalt(II) oxide (CoO) has been used as an anode catalyst in a direct borohydride fuel cell (DBFC). The microstructure of CoO has been characterised by X-ray diffraction. The cell performance and short-term performance stability of the DBFC using the CoO as anode catalyst have been investigated. At the optimum conditions, the maximum power density of 80 mW cm^{-2} has been achieved at 30 °C for this cell without using any precious metals and ion exchange membranes. Results from XRD, TEM, and XPS analysis confirm that the good performance of the fuel cell is attributed to the co-operation of CoO and CoB which formed from CoO during the operation.

1. Introduction

With the consumption of fossil-fuel resources, environmental pollution and global warming, there has been a strong awareness for both the research and use of more efficient and cleaner power sources. Fuel cells, which directly convert chemical energy into electrical energy with a high efficiency and low/zero-emission, have attracted much attention. The direct borohydride fuel cell (DBFC) is an interesting liquid type fuel cell due to its high energy density, low toxicity of borohydride, good power performance and the feasibility of using non-noble metals as both anode and cathode catalysts [1–3]. The reaction for DBFC is based on the borohydride oxidation and the oxygen reduction:

$$\text{Anode}: \quad BH_4^- + 8OH^- = BO_2^- + 6H_2O + 8e^- \quad E^0 = -1.24\,V \qquad (1)$$

$$\text{Cathode}: \quad 2O_2 + 4H_2O + 8e^- = 8OH^- \quad E^0 = 0.40\,V \qquad (2)$$

$$\text{Cell reaction}: \quad BH_4^- + 2O_2 = BO_2^- + 2H_2O \quad E^0 = 1.64\,V \qquad (3)$$

In recent years, many studies are carried out on the anode catalyst of DBFCs. The use of noble metals (platium, palladium and gold) [4–6], transition metals (nickel and copper) [7] and rare earth hydrogen storage alloys (AB_5- and AB_2-type alloys) [8–10] has been reported. The development of high performance electrode materials for fuel cells, however, is still one of the most attractive areas of electrochemical research. Presently, cobalt-based materials have been used in several types of the fuel cells [11–13]. For example, Jafarian et al. [14] use Co-based materials modified glassy carbon electrodes for electrocatalytic oxidation of methanol in DMFC and demonstrated good performance. Qin et al. [15] develop polypyrrole modified Co-based materials as cathode and anode catalysts in DBFC and achieve a maximum power density of 83 mW cm^{-2}. Moreover, some novel Co-based alloys, such as Co–B [16] and Co–Mo–B [17], have been applied successfully as catalysts for alkaline secondary batteries. Therefore Co-based materials are thought to be potentially good catalysts for cells, including DBFCs.

As is well known, cobalt(II) oxide (CoO) was used widely in various batteries although it merely acted as a battery additive. In our previous work, we also used CoO as an additive of the anode materials in DBFCs [18,19], but it was brought to our attention by accident. When we increased the quantity of CoO we noticed that the electrochemical properties of the working electrodes were also improved. Therefore, we chose to apply CoO as an anodic catalyst in a DBFC with $LaCoO_3$ as the cathodic catalyst. The properties of the single cell were investigated. The resultant DBFC shows an acceptable output power density (80 mW cm^{-2} at 30 °C) and stability without using any precious metals and ion exchange membranes.

2. Experimental details

2.1. Materials

Cobalt(II) oxide (CoO), analytical grade, was purchased from J&K Chemical Ltd. Hydrogen storage alloy (HSA), $MmNi_{3.55}Co_{0.75}Mn_{0.4}Al_{0.3}$ (where Mm denotes a Ce-rich mixed mischmetal composed of 50 wt.% Ce, 30 wt.% La, 5 wt.% Pr and 15 wt.% Nd) alloy, was purchased from Xiamen Tungsten Co., Ltd. Perovskite-type oxide ($LaCoO_3$) was prepared following the sol–gel method described by our previous works [18]. Lanthanum nitrate ($La(NO_3)_3{\cdot}6H_2O$), cobalt nitrate ($Co(NO_3)_2{\cdot}6H_2O$), citric

* Corresponding author. Tel.: +86 29 8266 4602; fax: +86 29 8266 3453.
E-mail addresses: lisai321@sina.com (S. Li), ynliu@mail.xjtu.edu.cn (Y. Liu).

0378-7753/$ – see front matter.
doi:10.1016/j.jpowsour.2010.05.016

acid ($C_6H_8O_7H_2O$), and ammonia water (NH_3H_2O) were all of analytical grade purity.

2.2. Electrode preparation

To prepare the anode, cobalt(II) oxide (CoO) powder (97 wt.%) was mixed together with 30% polytetrafluoroethylene (PTFE) solution (3 wt.%), and then the mixture was smeared onto a 1 cm × 1 cm Ni-foam sheet (thickness = 1.7 mm, porosity > 95%). After drying at 80 °C under vacuum for 2 h the electrode was pressed with a pressure of 3 MPa. The HSA anode was prepared by a similar method in order to contrast with the CoO anode. A blank test showed that the effect of Ni-foam sheet supporter on electrochemical performance of the fuel cell was negligible.

The cathode was a sandwich construction consisting of a gas diffusion layer, an active layer and a current accumulating matrix. The active layer was prepared by mixing 30 wt.% $LaCoO_3$ and 45 wt.% activated carbon with a 25 wt.% polytetrafluoroethylene (PTFE) emulsion and then coated onto a Ni-foam. The gas diffusion layer was prepared by mixing 60 wt.% acetylene black (with surface area 2500 $m^2\ g^{-1}$) and 40 wt.% PTFE with ethanol into 0.3-mm thick film. The three-layer gas electrode was finished by pressing the coated Ni-foam and the gas diffusion layer at 3 MPa into a 0.6-mm thick sheet.

2.3. Characterisation of the catalysts

X-ray diffraction (XRD) patterns of the samples were recorded in the 2θ range 10–80° with a RIGAKU D/MAX-2400 diffractometer using a CuKα (λ = 1.5444 Å) source. The microstructures were observed by transmission electron microscopy (TEM, JEM-2100F). X-ray photoelectron spectroscopy (XPS) measurements were carried out on a VG scientific MultiLab ESCA2000 instrument. The spectra were recorded using monochromatic AlKα radiation ($h\nu$ = 1486.60 eV) as the excitation source. Low-resolution spectra were recorded to determine the elements present in the sample and high-resolution spectra were recorded for Co2p and B1s levels to determine the chemical state of these elements. During the XPS experiments, the pressure inside the vacuum system was maintained at 1×10^{-9} Pa. Before analysis, the samples were dried under vacuum at 80 °C overnight.

2.4. Experimental set-up and procedure

The polarisation was employed to characterise the optimum conditions of anode using a computer controlled Electrochemistry Workstation CHI650 (Chenhua, Shanghai, China) with a conventional three-electrode configuration. The anode served as the working electrode. A Hg/HgO/6 M KOH electrode was used as a reference electrode, and a Pt wire was used as a counter electrode. An anode with an active area of 1 cm^2 was placed on a window on one side of the middle container. The reference electrode was connected to the body of the cell through a Luggin capillary, with the tip positioned close to the working electrode. The counter electrode (Pt wire) was placed on the other side of the container 2 cm away from the working electrode. The anode container was separated from the other containers by Nafion 117 membranes. The anolyte was prepared by dissolving KBH_4 in 6 M KOH or $NaBH_4$ in 6 M NaOH. The electrolyte in the outside compartments was either 6 M KOH or 6 M NaOH.

The discharge performances of the single DBFC were measured by a battery testing system (from Neware Technology Limited, Shenzhen, China). The cell testing system is shown in Fig. 1. The anode was placed on the inside of the container, and the cathode was placed on the window of the other side of the container. The gas diffusion layer of the cathode was exposed to air, whereas the active layer was in contact with the electrolyte fuel that was fed through a pump. The anode was 2 cm away from the cathode.

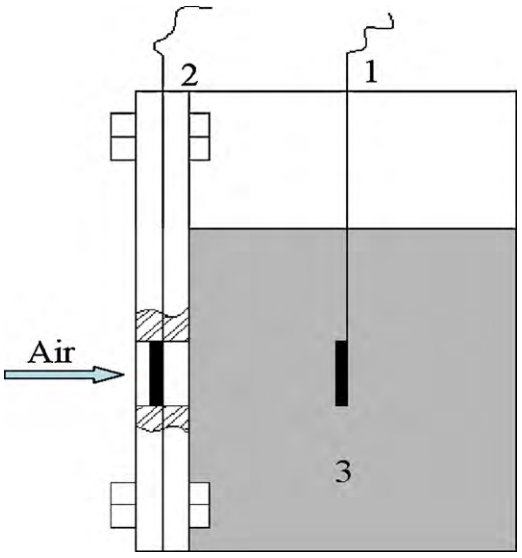

Fig. 1. Schematic diagram of single cell test system: (1) anode, (2) cathode, and (3) 0.8 M KBH_4–6 M KOH electrolytic fuel.

3. Results and discussion

3.1. Structural characterisation

Fig. 2 shows the X-ray diffraction (XRD) pattern of the CoO sample. The diffraction pattern confirmed that the CoO oxide is the only phase, and the XRD spectrum of CoO matched with the face-centred cubic (FCC) system as discussed earlier (PDF card no. 09-0402).

3.2. Influence of catalyst loadings on anode properties

For the fuel cell performance, the catalyst loading is an important influencing factor. The CoO catalyst anodes with different loading quantities were studied, as shown in Fig. 3. As the loadings increase from 0.006 g cm^{-2} to 0.14 g cm^{-2}, the polarisation decreases gradually. The current density shifts from 0.623 A cm^{-2} to 1.43 A cm^{-2} (at −0.8 V versus the Hg/HgO electrode), but the current density increases significantly between loadings of

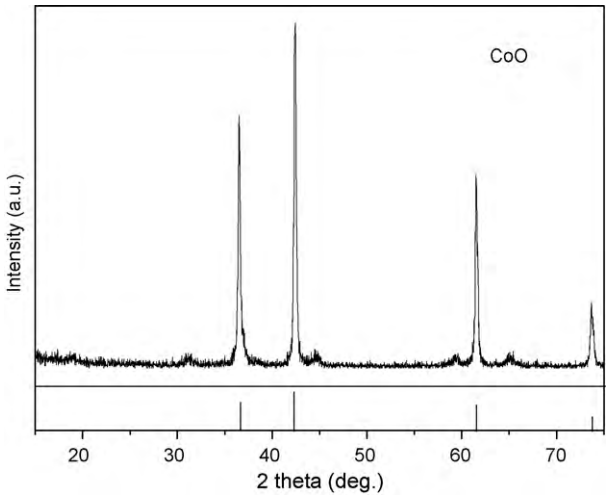

Fig. 2. XRD pattern of CoO.

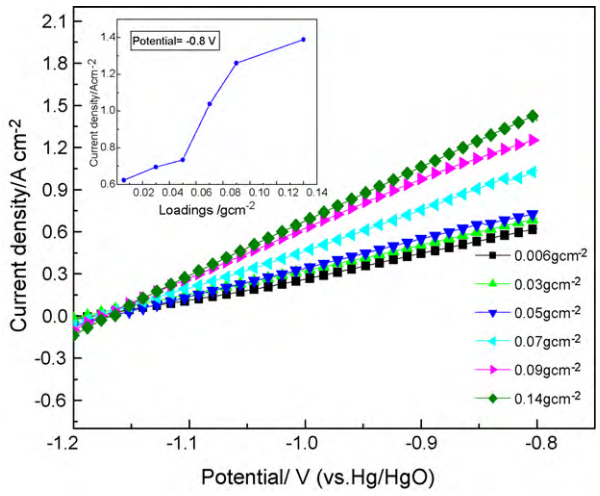

Fig. 3. Influence of CoO loadings on electrode properties. Electrolyte fuel is 0.8 M KBH_4–6 M KOH, scan rate is 10 mV s^{-1}.

0.05 g cm^{-2} and 0.09 g cm^{-2}. The increase in current density was moderate when the loadings less than 0.05 g cm^{-2} or greater than 0.09 g cm^{-2}. The reason may be that the less loading will affect the catalytic effect, while the larger loading will cause the adverse effect of the thick catalyst layer on resistance and mass transport of BH_4^-. The optimisation of catalyst loading led to an ideal value of 0.07 g cm^{-2}.

3.3. Influence of borohydride concentration on anode properties

In DBFC systems, the performance of cell greatly depends on the KBH_4 concentration in the electrolyte fuel. Fig. 4 shows the CoO-catalysed anode polarisation curves relative to the KBH_4 concentration from 0.1 M to 1.0 M in the 6 M KOH solutions at ambient atmosphere. As it can be seen from Fig. 4, the current densities are enhanced by increasing the KBH_4 concentration from 0.1 M to 0.8 M. Increases were not observed when the KBH_4 concentration is higher than 0.8 M, indicating the polarisation became stable when the borohydride concentration was increased to a certain level. Fig. 4 also displays a good linear relationship between potential and current density at high concentrations (0.8 M and 1.0 M). That is to say, there are no obvious activation polarisation and concentration polarisation in the reaction system, which could be attributed to the presence of ion balance in the electrode/electrolyte at high

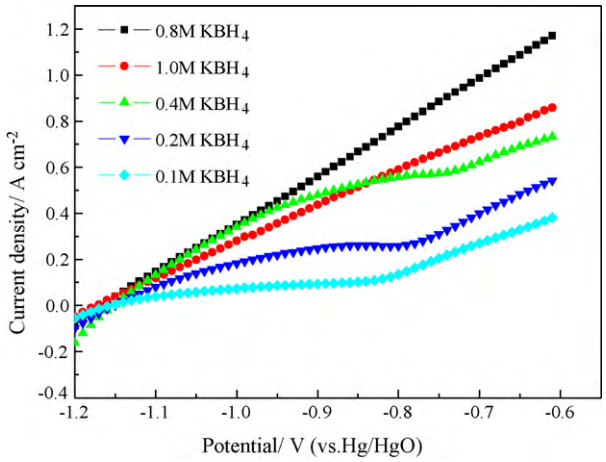

Fig. 4. Influence of KBH_4 concentration on CoO-catalysed anode in 6 M KOH solution at ambient atmosphere. Catalyst loading is 0.07 g cm^{-2}, scan rate of 10 mV s^{-1}.

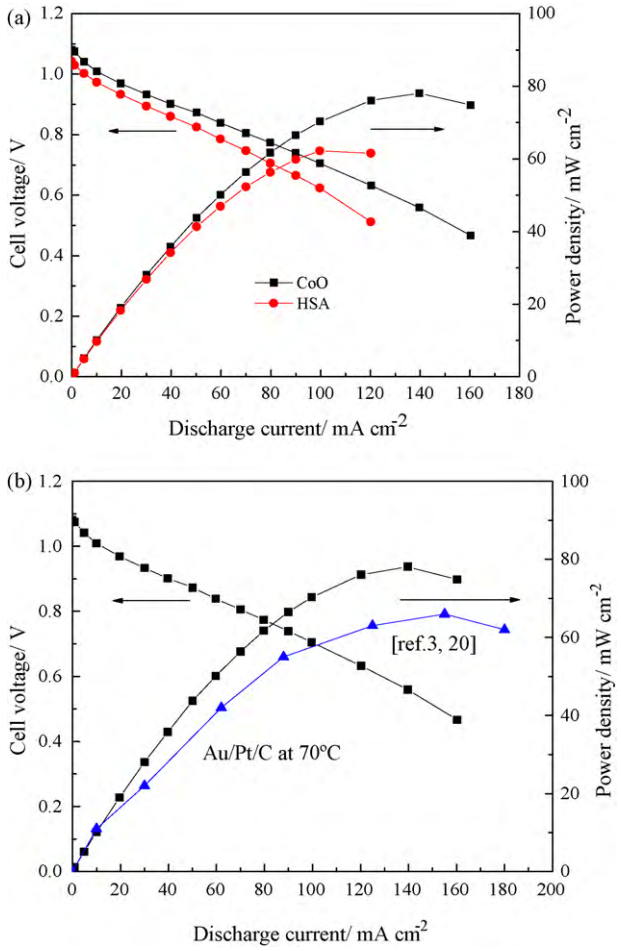

Fig. 5. Performances of the DBFCs. (a) CoO and HSA as anode catalysts, respectively, and $LaCoO_3$ as cathode catalyst at 30 °C. (b) Referenced cell performance using Au/Pt/C as anode catalyst at 70 °C [3,20]. Anode: CoO loading is 0.07 g cm^{-2}. Cathode: $LaCoO_3$ loading is 0.0075 g cm^{-2}. Electrolyte fuel is 0.8 M KBH_4–6 M KOH.

concentration [19]. However, as shown in Fig. 4, when the concentration of KBH_4 is less than 0.4 M, there are obvious nonlinear polarisation curves, suggesting that in addition to ohmic polarisation, the concentration polarisation effects were also very serious at low concentration. So the electrolyte fuel of 0.8 M KBH_4–6 M KOH is selected in the research.

3.4. Fuel cell performances

We constructed two test cells using the CoO and HSA as anode catalysts, respectively, and $LaCoO_3$ as cathode catalysts. Whether the precious ion exchange membrane should be used in the cell depends on the borohydride tolerance of the cathode. In previous work, we have shown that $LaCoO_3$ exhibited good catalytic activity for the oxygen reduction reaction (ORR) and good borohydride poison tolerance [18]. Thus, in this work, a DBFC structure was designed with no membrane. The performances of the cells using CoO and HSA as anode catalysts at different discharge current densities are shown in Fig. 5(a). Compared with the cell using the HSA as anode catalyst, the cell using CoO demonstrated a higher performance. A maximum power density of 80 mW cm^{-2} was achieved at 0.57 V. However, the maximum power density was only about 62 mW cm^{-2} when using the HSA as anodic catalyst under the same conditions. The steady-state polarisation curves also displayed that the voltage and the current densities have a linear relationship, the slope of the linear of the CoO anode was noticeably lower than

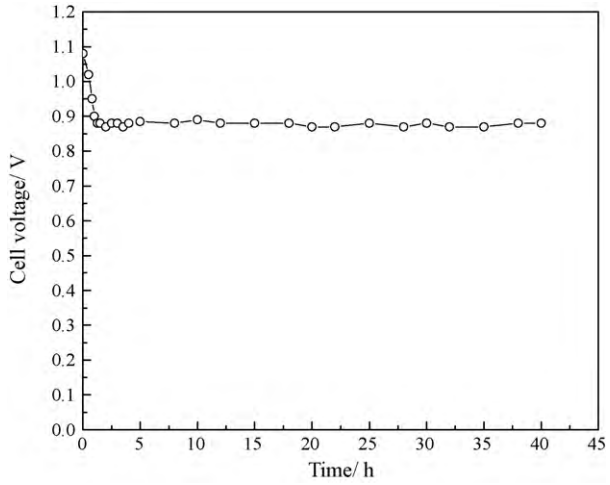

Fig. 6. Stability test of the DBFC using CoO anode operating at a current density of 50 mA cm^{-2} at ambient conditions.

that of the HSA anode, suggesting that the CoO electrode has better electrochemical performance. In addition, Fig. 5(b) also shows the power density of noble metals Au/Pt/C catalysed anode in a DBFC reported in Refs. [3,20]. As shown in Fig. 5(b), the maximum power density was about 60 mW cm^{-2} at 70 °C. The CoO anode has an acceptable electrochemical performance in comparison with precious metals anode (Au/Pt/C).

The DBFC performance stability was tested by monitoring voltage changes in the cell during galvanostatic discharge. Fig. 6 shows the changes in cell voltage at a constant current discharge of 50 mA cm^{-2} continued for about 40 h at ambient atmosphere. As shown in Fig. 6, despite some slight changes, attenuation was not observed within 40 h, suggesting that the cell using CoO as the anode catalyst has good performance stability.

3.5. Characterisation of the catalyst after tests

To understand the function of CoO as an anode catalyst in the DBFC, its microstructure was examined by XRD and TEM after the experiments. The used catalyst powder was washed with plenty of DI water to remove the potassium metaborate solution, and dried at 80 °C under vacuum. For the convenience of comparison, the XRD patterns of as such sample and that for the sample used in the experiments are presented in Fig. 7 . It was found that the sample after use in experiments showed only a broad diffraction peak near $2\theta = 45°$, approaching an amorphous material. The diffraction peaks of crystalline CoO were absent. The results coincide with the amorphous nature of Co–B [21]. Fig. 8 shows a TEM image and

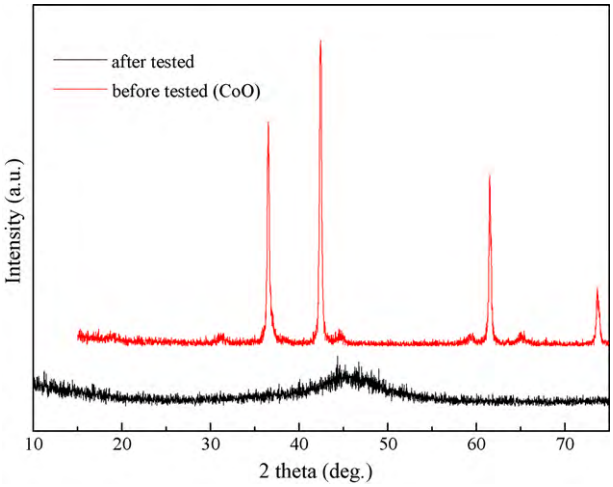

Fig. 7. XRD patterns of CoO before and after tests.

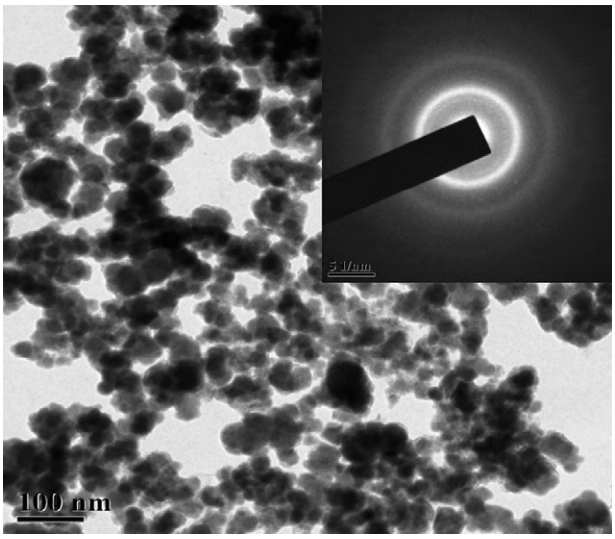

Fig. 8. TEM image of CoO sample after use in the experiments.

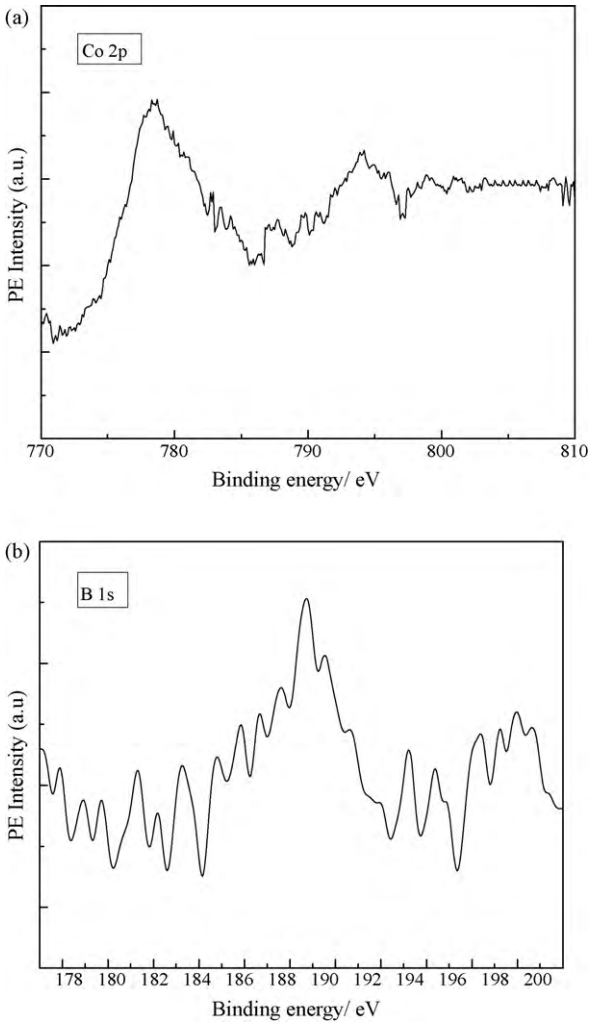

Fig. 9. XPS spectra of CoB formed from CoO in experiments (a) Co2p spectra and (b) B1s spectra.

corresponding selected area diffraction (SAD) pattern of the sample used in the experiments. The diffused ring in the SAD pattern also reconfirmed the presence of amorphous phase for the used sample.

Considering that CoB could not be ascertained by XRD and TEM due to its amorphous state, the CoB powder formed from CoO during the experiments was washed, dried and analysed by XPS. Fig. 9 displays the XPS spectra of Co2p and B1s for the amorphous CoB. The binding energy of 778.70 eV observed for $Co2p_{3/2}$ is within the range of 778–780.4 eV reported for $Co2p_{3/2}$ in the CoB catalysts [22,23], and the binding energy of 188.85 eV for B1s is close to the reported 188.73 eV [22] and 187.8 eV [23] in CoB catalysts. The XPS results ultimately proved the amorphous material formed during the experiments is CoB. Thus, for the anode catalytic, it was presumed that the catalytic action would be the co-operation of CoO and CoB.

4. Conclusions

In this paper, the CoO catalyst was used as the anodic catalyst in a DBFC. Compared with the cell using the HSA or some precious metals (Au/Pt/C) as anodic catalysts, the cell using CoO demonstrated a higher discharge performance. At the optimum conditions, the maximum power density of 80 mW cm^{-2} was obtained for this cell at 30 °C. Furthermore, the DBFC displayed good short-term durability with CoO as the anodic catalyst. It was found that the acceptable catalytic properties observed with CoO were attributed to the co-operation of CoO and CoB which formed from CoO during the experiments.

References

[1] J. Ma, N.A. Choudhury, Y. Sahai, Renew. Sustain. Energy Rev. 14 (2010) 183–199.
[2] U.B. Demirci, J. Power Sources 172 (2007) 676–687.
[3] C. Ponce de Leon, F.C. Walsh, D. Pletcher, D.J. Browning, J.B. Lakeman, Int. J. Hydrogen Energy 155 (2006) 172–181.
[4] M.H. Atwan, C.L.B. Macdonald, D.O. Northwood, E.L. Gyenge, J. Power Sources 158 (2006) 36–44.
[5] J.L. Wei, X.Y. Wang, Y. Wang, Q.Q. Chen, F. Pei, Y.S. Wang, Int. J. Hydrogen Energy 34 (2009) 3360–3366.
[6] X.Y. Geng, H.M. Zhang, W. Ye, Y.W. Ma, H.X. Zhong, J. Power Sources 185 (2008) 627–632.
[7] B.H. Liu, Z.P. Li, S. Suda, Electrochim. Acta 49 (2004) 3097–3105.
[8] L.B. Wang, C.A. Ma, X.B. Mao, J.F. Sheng, F.Z. Bai, F. Tang, Electrochem. Commun. 7 (2005) 1477–1481.
[9] B.H. Liu, S. Suda, J. Alloys Compd. 454 (2008) 280–285.
[10] Z.Z. Yang, L.B. Wang, Y.F. Gao, X.B. Mao, C.A. Ma, J. Power Sources 184 (2008) 260–264.
[11] J.Y. Liang, Y.L. Li, Y.Q. Huang, J.Y. Yang, H.L. Tang, Z.D. Wei, P.K. Shen, Int. J. Hydrogen Energy 33 (2008) 4048–4054.
[12] I. Zacharaki, C.G. Kontoyannis, S. Boghosian, A. Lycourghiotis, C. Kordulis, Catal. Today 143 (2009) 38–44.
[13] C.H. Liu, B.H. Chen, C.L. Hsueh, J.R. Ku, F.H. Tsau, K.J. Hwang, Appl. Catal. B 191 (2009) 368–379.
[14] M. Jafarian, M.G. Mahjani, H. Heli, F. Gobal, H. Khajehsharifi, M.H. Hamedi, Electrochim. Acta 48 (2003) 3423–3429.
[15] H.Y. Qin, Z.X. Liu, L.Q. Ye, J.K. Zhu, Z.P. Li, J. Power Sources 192 (2009) 385–390.
[16] D.G. Tong, Y.Y. Luo, W. Chu, Mater. Chem. Phys. 112 (2008) 907–911.
[17] X.F. Chen, H.X. Li, H.S. Luo, M.H. Qiao, Appl. Catal. A 233 (2002) 13–20.
[18] Y. Liu, J.F. Ma, J.H. Lai, Y.N. Liu, J. Alloys Compd. 488 (2009) 204–207.
[19] J.F. Ma, J. Wang, Y.N. Liu, J. Power Sources 172 (2007) 220–224.
[20] S.C. Amendola, P. Onnerud, P.T. Kelly, P.J. Petillo, S.L. Sharp-Goldman, M. Binder, J. Power Sources 84 (1999) 130–134.
[21] A. Garron, D. Swierczynski, S. Bennici, A. Auroux, Int. J. Hydrogen Energy 34 (2009) 1185–1199.
[22] P. Krishnan, K.L. Hsueh, S.D. Yim, Appl. Catal. B 77 (2007) 206–214.
[23] H. Ma, W.Q. Ji, J.Z. Zhao, J. Liang, J. Chen, J. Alloys Compd. 474 (2009) 584–589.